Title
Applying flow convergence routing to control sediment erosion and deposition locations in a dam's backwater zone

Authors
Li, Tingyu
Pasternack, Gregory B

Publication Date
2023-08-01

DOI
10.1016/j.geomorph.2023.108882

Geomorphology 440 (2023) 108882

Contents lists available at ScienceDirect

Geomorphology

journal homepage: www.journals.elsevier.com/geomorphology

Applying flow convergence routing to control sediment erosion and deposition locations in a dam's backwater zone

Tingyu Li, Gregory B. Pasternack *

Department of Land, Air and Water Resources, University of California at Davis, CA, USA

ARTICLE INFO

Keywords:
Reservoir sedimentation
Topographic constriction
Flow convergence routing
Sediment erosion

ABSTRACT

Despite studies showing that dams have significant effects on the sediment dynamics and evolution of a river upstream of a dam, the knowledge of relationships between river topography and sediment transport in a dam's backwater zone has hardly been applied in reservoir sedimentation management. This study investigated the potential of an alternating sequence of engineered topographic nozzles and oversized landforms, utilizing flow convergence routing theory, to redistribute sediment erosion foci in a dam's backwater zone for remote mountain reservoirs with a sediment storage capacity of ~10^5 m^3. To test scientific ideas and engineering alternatives, the current topography of the backwater zone upstream from Our House Dam on the confined, mountainous Middle Yuba River, California, was virtually re-contoured into different scenarios for numerical experimentation. As most of the dam's backwater zone is filled with sediment (a common global problem) in a narrow, confined canyon, two-dimensional hydrodynamic modeling was useful for evaluating erosion patterns resulting from different manipulations. The results found that high velocity concentrates through nozzles and dissipates through oversized landforms, resulting in the latter exhibiting hydraulics indicative of functioning as sediment settling basins. These basins can be located away from the dam where key infrastructure needs clearance from sedimentation. As flow increases through the sequence of nozzles and oversized landforms, each nozzle's hydraulic jet will persist farther into the oversized area. Moderate in-channel flow (daily recurrence of ~5–30 %) was best for creating conditions to force deposition of sediment in oversized landforms. At high enough discharge (recurrence of <1–5 %) significant sediment erosion can occur throughout the constructed terrain in the backwater zone, so the whole topographic scheme can become overwhelmed and ineffective. Thus, the performance of re-contouring as an aid in reservoir sedimentation management is location and flow-dependent, necessitating careful design refinement for local conditions and assessment of financial benefits and costs. Overall, this study opens a new realm of sediment management for dam operators and regulators hard-pressed to know what to do when a moderate-sized mountain reservoir with poor accessibility has a sediment storage capacity of ~10^5 m^3.

1. Introduction

Reservoir sedimentation is the term used to describe the processes of erosion, entrainment, transportation, deposition, and compaction of sediment delivered to and redistributed throughout the reservoir upstream of a dam (Morris and Fan, 1998; Julien, 2010; Li and Pasternack, 2022). Starting from sediment dynamics, incoming coarse sediment (bedload) derives from the upstream catchment and channel erosion. This material tends to deposit and form a delta at the head of the reservoir, while fine sediment deposits farther downstream in the reservoir (Hotchkiss and Parker, 1991). Consequently, a variety of morphological adjustments are triggered, such as lateral river migration, channel deepening and widening, morphological evolution of channel bars and grain-size partitioning along the channel axis (Maselli et al., 2018). Feedbacks also exist between sediment dynamics and morphological adjustment (Coleman, 1976; Liro, 2016). For example, large bars depositing in a wide channel may eventually act as a barrier to sediment transport (Hooke, 2003; Fryirs, 2013), thereby promoting upstream bar extension as the foci of deposition shifts farther upstream in response, as positive feedback (Schumm, 1985; Fryirs, 2013; Liro, 2015).

Reservoir sedimentation is especially problematic and difficult to address for older dams located in remote, confined mountain canyons and holding back ~10^5 m^3 of sediment for which excavation and/or bypass are not viable or cost-effective. For example, within the next

* Corresponding author.
E-mail address: gpast@ucdavis.edu (G.B. Pasternack).

https://doi.org/10.1016/j.geomorph.2023.108882
Received 27 January 2023; Received in revised form 21 August 2023; Accepted 21 August 2023
Available online 22 August 2023

several decades, many of California's reservoirs will approach the end of their anticipated design lifetime, while many others have already passed their anticipated design lifetime (Ho et al., 2017; Randle et al., 2021). As an extra complication, reservoirs behind small mountain dams in drier climates may be kept empty or only partially filled with water (by design or increasingly as an undesirable result of droughts exacerbated by anthropogenic climate change), exposing sediment fill and redistributing sediment right up against critical infrastructure at the dam. Specifically, this can cause a problem in which the entrances to low-level valves and diversion tunnels become clogged. Such infrastructure must be kept free of sediment to maintain environmental flow regimes below dams and to provide water transfers among different reservoirs.

Given the difficulty of these problems, highly creative solutions warrant development and consideration, stimulating the novel approach proposed herein. Specifically, in some locations, it may be feasible and cost-effective to direct erosion and deposition in a reservoir to beneficial locations by mindful control of the morphodynamic mechanism of flow convergence routing (described next). This work is scientifically meaningful and societally valuable because it explored the possibility of extending the life of dams with a holding capacity of $\sim 10^5$ m^3 of sediment (typically too much to repeatedly excavate and permanently store) through sediment re-contouring and alternative management practices, instead of through enormous and expensive sediment removal, flushing, or bypassing programs.

1.1. Flow convergence routing

Topographic steering is defined as morphological control of water depth, speed and direction (i.e., hydraulics) (Blanckaert, 2011; Nelson and Dubé, 2016). The term is used by some engineers to refer exclusively to a fluid mechanics phenomenon, but increasingly, geomorphologists and river restoration practitioners are adapting it to refer to a more literal concept in which fluvial landforms and large bed elements control hydrodynamics (Brown and Pasternack, 2014). As an example, materials in transport can be directed into persistent topographic depressions or up against immobile large bed elements creating deposits caused by particle trapping (Brown et al., 2016). Common fluvial topographic steering features include gravel/cobble bars, bedrock outcrops, wood jams, and large bed elements.

Flow convergence routing (FCR) is a thoroughly studied hydromorphodynamical mechanism associated with topographic steering. Flow convergence relates to the fluid mechanism and routing relates to its sediment dynamics. Locations of the most concentrated flow (i.e., geometric constrictions termed “nozzles”) at any discharge have the greatest potential to scour and route sediment through them (MacWilliams Jr et al., 2006; Pasternack et al., 2018a). In contrast, locations of the least concentrated flow at any discharge (generally “oversized” cross sections compared to average dimensions) have flow divergence and the highest likelihood of sediment deposition at that flow (i.e., functioning as sedimentation basins). Most importantly, these locations of least and most concentrated flow (and the deposition and erosion they drive) can shift as a function of discharge, because smaller fluvial landforms are often nested within larger fluvial landforms with different topographic steering (Pasternack et al., 2018b, 2021). While flow convergence routing has been studied in a growing number of natural fluvial rivers (e.g., Byrne et al., 2021), and it has been used to design river rehabilitation projects (e.g., Wheaton et al., 2010; EPA, 2020; Collison, 2016), this study presents the first conceptualization and experimental testing of its potential for use in managing reservoir sedimentation under appropriate conditions.

1.2. Scientific questions and hypotheses

We posit a new way to manage reservoir sedimentation, especially where wholesale excavation is too expensive or infeasible. Specifically, we propose that in some circumstances dam operators could re-contour deposited sediment (thereby saving the cost of excavation and removal) to control where and when existing sediment in the reservoir erodes to move farther downstream as well as where and when new sediment deposits in the future. As a one-time action, this approach only mitigates the sedimentation problem for a period, until the locations designed to store new deposits fill up. However, using this strategy, the smaller amount of future sediment deposition could be directed to specific focused locations easier to excavate on an on-going basis. In that case, then this strategy can provide a long-term solution. The details of what is possible depend on local site conditions and finances. This approach is most likely to be successful where coarse sediment sizes comprise most of the deposit in order to maintain the integrity of re-contoured landforms. Exactly where a dam operator wants to focus erosion or deposition may vary.

The overall goal of this study is to present the theoretical concept of controlling foci of erosion and deposition in a reservoir's backwater zone and explore the concept's potential by answering specific scientific questions using a virtual test case based on a real site in California. In this study, the focus of virtual site design was on avoiding deposition at the dam where low-level valves need to be kept free of sediment, and instead directing sediment to two zones upstream. Three scientific questions were posed to analyze impacts of topographic constriction and stage drawdown on reservoir sediment erosion, the optimal range of hydrologic conditions, and the mechanistic sequence of hydrodynamics triggered by re-contouring.

Qt1. How do topographic controls involving wide, deep (i.e., oversized) and narrow, shallow (i.e., nozzle) landforms affect foci of sediment erosion, and by inference foci of deposition?

Qt2. How does topographic adjustment function together with different amounts of water surface elevation (WSE) drawdown to affect sediment erosion, and by inference foci of deposition?

Qt3. What are optimal hydrologic conditions for constructed topographic controls to focus erosion potential in nozzle landforms, and by inference sediment focus deposition in oversized landforms?

The topographic control is a set of two topographic nozzle landforms (TPC1 & TPC2) and a topographic oversized landform between nozzles (Fig. 1). Although not re-contoured, the section upstream of TPC2 may also be an oversized landform, depending on channel and reservoir topography. Landform terminology comes from FCR theory (Pasternack et al., 2018a). According to theory, nozzles and oversized landforms are not naturally self-sustainable in the face of morphodynamics, unless a nozzle is highly resistant to erosion, such as if its lithology is highly resistant bedrock. However, a nozzle can be engineered for persistence as a hard structure, and that would be anticipated for TCP1 and TCP2, ideally using the coarser fraction of on-site deposits.

Engineered FCR is hypothesized to be capable of manipulating the spatial distribution of sediment erosion in a reservoir to shift the foci of erosion away from critical dam infrastructure. Under this hypothesis, TPC2 ought to yield a convergent and accelerated flow at the head of the oversized landform between TPC2 and TPC1; which generates a hydraulic jet through and downstream of the nozzle, causing erosion and making new foci of sediment erosion. Therefore, TPC2 is assumed to accelerate flow and deliver more sediment to the oversized landform downstream of it. Meanwhile, even though TPC1 is a nozzle with high transport capacity inside of it, it is hypothesized to have a low possibility of transporting sediment because of a lack of sediment supply routing to it, given the upstream oversized landform acting as a settling basin. TCP1 serves as a backstop to sediment transport by backing water up into the oversized landform, thereby further reducing the overall dynamism. While the channel expands again leading up to the reservoir itself, TCPs 1 and 2 are designed to be able to capture incoming sediment before it can get to the final expansion. Further design refinement in a real application could adjust this last area in front of the dam to meet project specifications as needed.

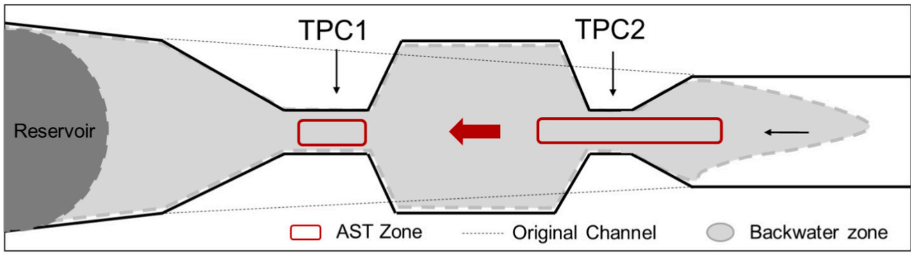

Fig. 1. Conceptual configuration of topographic controls in a reservoir backwater zone. AST is active sediment transport.

TPC performance is hypothesized to be sensitive to the downstream WSE imposed by the reservoir. Lowering WSE can reduce the ponding/backwater effect of the reservoir and thus increase sediment erosion in TPC2 and the oversized landform. In that condition with more eroded sediment upstream, sediment erosion in TPC1 is hypothesized to increase without sufficient armoring, which would be detrimental. Conversely, increasing WSE can increase the ponding/backwater effect of the oversized landform and thus reduce sediment erosion potential in TPC2. By having less sediment transport to and through the oversized landform, sediment deposition near the dam can be reduced. Meanwhile, lower velocities throughout the reservoir, induced by the enhanced backwater effect, can reduce sediment erosion close to the dam. Both changes support of overall stability of any critical infrastructure present at the dam, such as low-level valves. Even though impacts of WSE adjustment can be independent of inflow to the extent that outflows can be manipulated to enforce the designated reservoir WSE, it can be no longer controllable beyond certain high discharge. Therefore, the effectiveness of TPCs is hypothesized to be flow dependent. When discharge reaches a certain high range, the performance of TPC1 is hypothesized to act as an accelerator to increase sediment transport through/over the reservoir because of the submergence of TPC2, depending on the infrastructure at the dam.

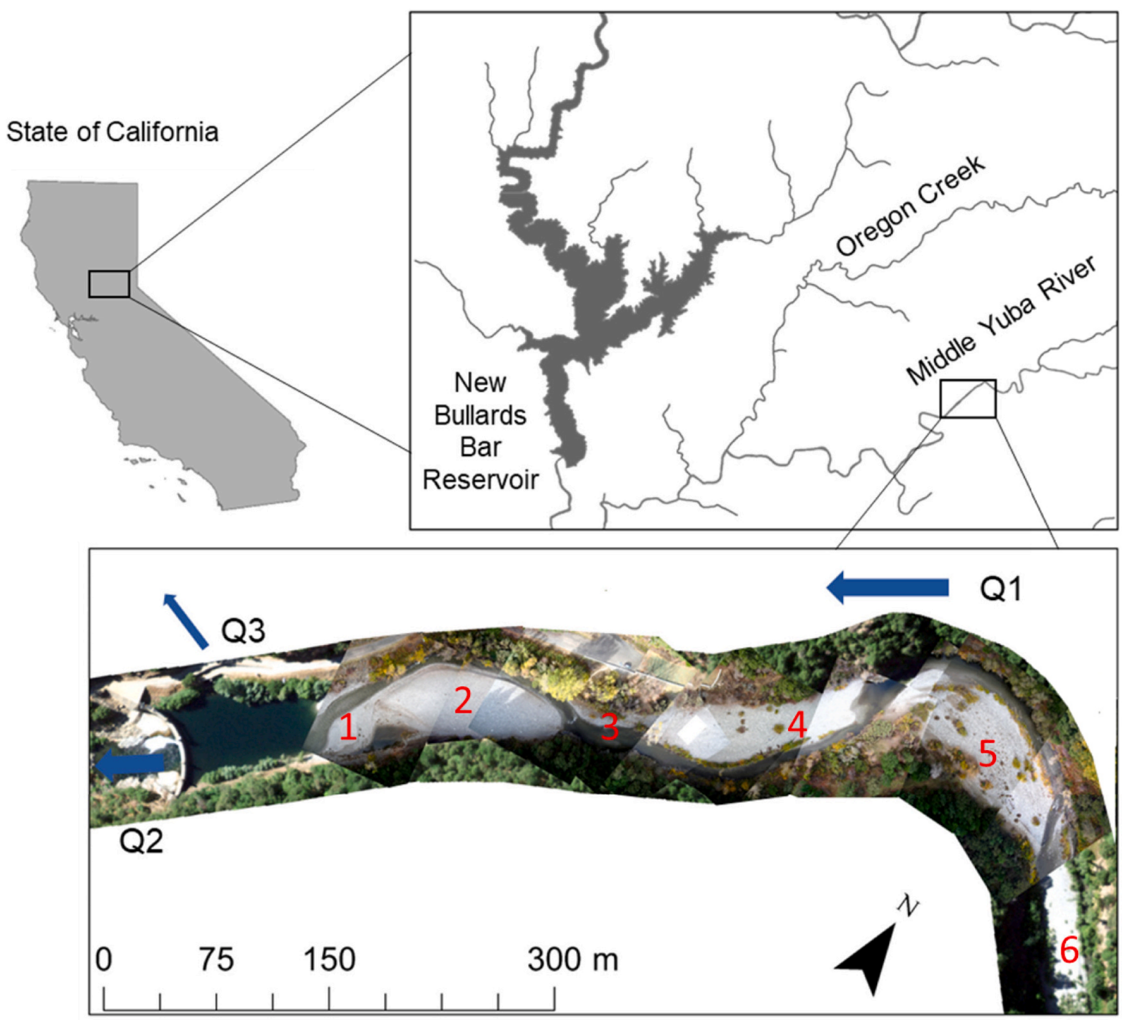

Fig. 2. Map of California, USA. Zoomed map of partial Yuba River catchment showing Middle Yuba River. Aerial imagery of the study reach. Q1 and Q2 are Middle Yuba River inflow and outflow, respectively. Q3 is water diverted through Lohman Ridge Tunnel.

2. Study site

In theory, the study questions could be answered with an entirely hypothetical set of topographic and hydrological scenarios (e.g., Brown et al., 2016), but it is often helpful to use a real site with real, typical river management problems as a testbed (e.g., Wheaton et al., 2010). The study site used herein was the backwater zone upstream of Our House Dam (OHD), a 40-m-radius concrete arch dam located 19 km upstream of the confluence of Middle Yuba River (MYR) and North Yuba River (Fig. 2). The dam is 21 m high with a crest length of 112 m and a crest elevation of 625 m above mean sea level. It is a diversion dam that conveys a maximum flow of 24.4 m^3/s from the MYR through its 6-km length to Oregon Creek. The diversion dam has a spillway capacity of 170 m^3/s.

Middle Yuba River at OHD has a drainage area of 376 km^2, with divide elevations as high as 2550 m (YCWA, 2017). According to the State Geologic Map Compilation geodatabase of the conterminous United States (https://doi.org/10.5066/F7WH2N65), there is a complex pattern of surficial metamorphic, igneous, and sedimentary bedrock types, including but not limited to Mesozoic volcanic and metavolcanic rocks, Paleozoic metasedimentary rocks, and Mesozoic granite. Most importantly, there is an abundance of Tertiary deposits of gravel, large boulders, and sands that were rich in gold. These became the focus of hydraulic gold mining in the late nineteenth century, which overwhelmed the river corridor with sediment (Gilbert, 1917). During the last century, MYR passed a lot of its stored mining sediment downstream, so by now its reaches are predominantly classified as “confined, boulder, high gradient, step-pool/cascade”, according to the Sacramento River regional river classification system (Byrne et al., 2020).

The catchment's climate is Mediterranean-montane, with warm, dry summers and cool, wet winters. Annual precipitation of 500–2000 mm varies with elevation and aspect. Winter flood pulses often stem from narrow-banded atmospheric rivers that deliver localized, intense, high-magnitude precipitation (Ralph et al., 2006; Dettinger, 2011). The catchment also periodically experiences low pressure systems and “bomb cyclones” that can deliver moderate to heavy precipitation over an extended duration.

Hydrologically, MYR is the only inflow to OHD (Fig. 2). The mean annual flow of MYR is 8.8 m^3/s. Recent instantaneous flood peak discharges were 405 m^3/s in 2017, 501 m^3/s in 2006, and 779 m^3/s in 1997. Inflow at OHD is partially diverted to Oregon Creek through the Lohman Ridge Tunnel. Lohman Ridge Diversion Tunnel conveys a maximum flow of 24.4 m^3/s.

Vegetation in the MYR catchment is predominantly conifer forest and there is streamwood present (YCWA, 2014). Some patches of hardwoods are present in and on the hillsides of the river corridors (Fites-Kaufmann et al., 2007). Riparian vegetation is present in the flood-prone width, Such as white alder, black locust, and various willow species. Wildfire is another major disturbance in the region, and it produces a variety of intensities, burn areas, and patterns (CAL FIRE, 2022). The largest one to affect the MYR catchment burned ~6583 ha in 1924. As a result of wildfire and other processes, there exists streamwood in the river corridor. Vaughan (2013) estimated that the 3480 km^2 Yuba catchment stores 600,500 m^3 of large streamwood. Senter et al. (2017) estimated that the North Yuba River exports 1.8–2.2 m^3/year/km^2, so when applied to the MYR catchment that could be 677–827 m^3/year arriving at OHD, with high interannual variability.

Channel dynamism and hillslope processes driven by this climate regime are the primary sources of sediment supply to OHD (Curtis et al., 2005). Historic hydraulic gold mining stored much sediment in the channel, with some residual still present (especially in headwaters), and it left large patches of unvegetated hillsides with easily erodible soils and loose sediment piles. MYR also has other areas of deforestation, roads, land use, and wildfire causing higher sediment yields (Lewis et al., 2006; Litschert and MacDonald, 2009; Olsen et al., 2021). Consequently, OHD experiences significant sediment deposition impairing operations for environmental flow releases.

The reach length affected by OHD (~1 km) was selected based on the distribution of subaerial gravel-bar deposition as an indicator of backwater extent (Fig. 2). It is a confined riffle-pool channel whose bed sediment is predominantly gravel and cobble, which then abruptly shifts to a noticeable amount of sand and silt among the gravel and cobble close to the dam (Fig. 3). The mean bed slope and width are 0.02 and 47 m, respectively. Hillsides are well vegetated, while the active riverbed is intermittently vegetated with willow species depending on the time since the last channel-altering flood.

3. Methods

3.1. Experimental design

This section presents an overview of the experimental design to show how specific, tractable scientific questions and their associated hypotheses (guided by a pre-existing mechanistic conceptualization) were tested, with details in subsequent methods sections. The design involved using an analytical and statistical framework (Fig. 4) for comparing three topographic-hydrological scenarios (Table 1) using two test metrics. Each metric has a pre-established range of values indicating the physical mechanisms in question. Comparisons of test metrics between H1 and H2 were used to answer Qt1, while those between H2 and H3 were used to answer Qt2. Comparisons of test metrics among different flows simulated for H1, H2, and H3 were used to answer Qt3.

In this study, the analytical methods focus on erosion, because its prediction is tractable using local shear stresses predicted with two-dimensional (2D) hydrodynamic modeling (Pasternack et al., 2006), which is a useful tool for this confined fluvial setting. Morphodynamic modeling was not used because the physical processes of sediment transport are extremely complex and thus far numerical modeling to directly simulate sediment transport is still under development, whereas this study just needed to characterize tendencies for erosion and sedimentation relative to TCP locations (see Section 3.4 for further justification). Further, model-predicted sediment transport rates are still markedly different from measured ones (Yager et al., 2018), questioning the viability of morphodynamic modeling for management use.

According to the literature and based on practitioner reports from river engineering projects designed with the aid of 2D modeling and analysis, 2D modeling has proven better at predicting erosion than deposition. For example, Rathburn and Wohl (2003) evaluated the performance of 2D-model-based erosion and deposition dynamics using an analytical framework like the one herein and found positive but mixed results, especially for deposition. They explained that the 2D-modeling shear stress approach is “overly simplified, predicting only particle motion or stability, rather than allowing for the simultaneous transport, aggradation, and degradation that accompany flow.” The concern is the lack of a specific shear stress range that is definitively depositional as opposed to just being stable, because deposition is first predicated on a sufficient sediment supply. In contrast, when the shields stress is in the active sediment transport range (defined in Section 3.4.1 below), then the sediment supply should be kept in transport and bed sediment can be eroded. These concepts are further supported by Sawyer et al. (2010), who found Shields stress thresholds for both erosion and deposition in a gravel-cobble reach where significant topographic change was present, but the thresholds did not necessarily work where topographic change was modest or absent. In other words, low shear stress was present in places of both deposition and no change. Overall, the revelation of spatially explicit, discharge-dependent hydraulics using 2D modeling helps quantify and interpret morphodynamic processes, and is more useful in interpreting erosion than deposition, so this study focuses its quantitative experimental design on erosion and relies on interpretation of hydraulics and FCR to assess deposition.

In H3–1 and H3–3, reservoir WSE was reduced by 0.6 and 2.9 m, respectively, to evaluate how WSE adjustment affects the TPCs

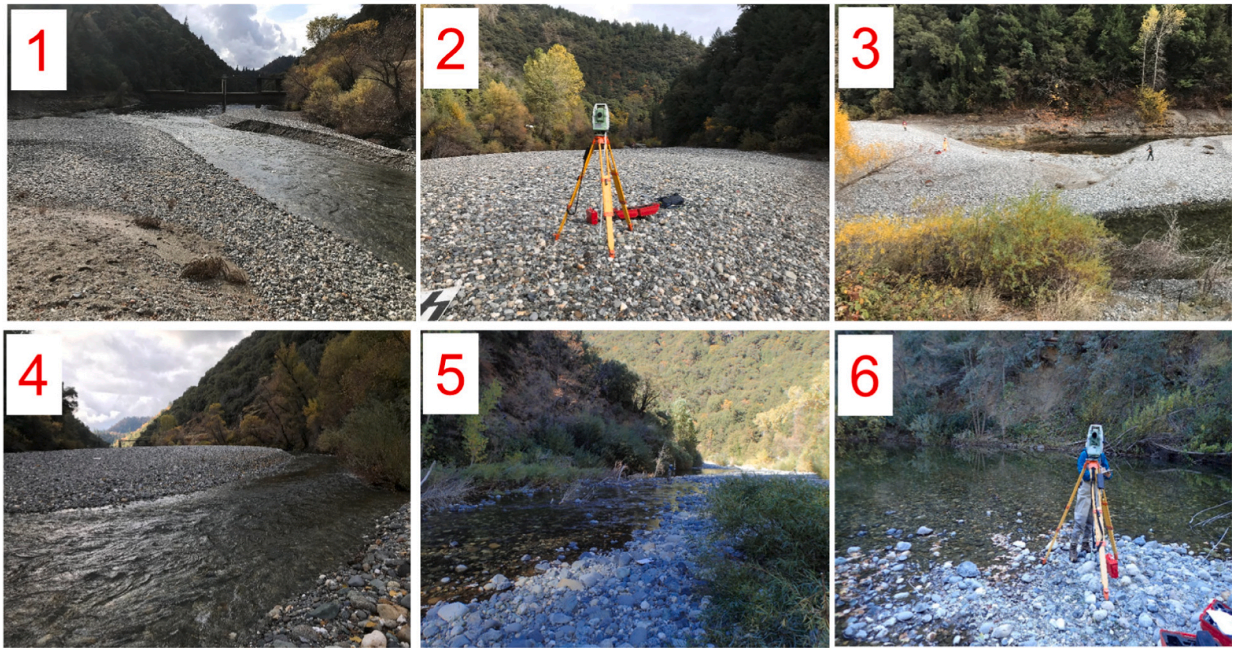

Fig. 3. Photos showing MYR and its substrates. Panel numbering increases in the upstream direction. Locations are marked in Fig. 2.

performance. In H3–2, WSE was increased by 0.3 m to evaluate the performance of TPCs with increased backwater effects. The minor WSE adjustment (−0.6 m and + 0.3 m) was set because the average WSE was close to the spillway height. Reducing reservoir by 2.9 m accounts for ¼ of the adjustable WSE range to evaluate how large adjustment affects TPCs performance. The adjustable WSE range is the difference between spillway height (619 m) and minimum WSE (607 m).

To obtain a robust understanding of baseline hydraulics, 2D hydrodynamic modeling (Section 3.3) of H1 was performed for 18 flow events (Table S1) considering the response of five representative grain sizes (3, 8, 32, 64 and 119 mm) to predicted bed shear stress, but then for brevity this study focused on evaluating conditions during three representative in-channel flows. To evaluate sediment dynamics, spatially explicit bed shear stress and flow depth rasters from 2D modeling were used to quantify scour potential (independent of sediment supply) and identify the location(s) where sediment erosion would happen relative to key infrastructure (Fig. 4). Two test metrics – the areal percentage of unstable riverbed (Section 3.4.1) and shortest distance of active transport from the dam (Section 3.4.2) – were computed and used to address the questions and hypotheses (Section 3.5).

3.2. Digital elevation model

A one-meter resolution DEM of the study site (Fig. 5A) was produced by combining points from airborne, ground, and bathymetric surveys after careful quality control/assurance measures. Tahoe National Forest 2014 airborne near-infrared Light Detection and Ranging (LiDAR) point cloud data (11.6 pts./m^2) were obtained from OpenTopography. Ground points were measured October to November 2018 using a Leica TPS1100 robotic total station and Trimble R8 Real-Time Kinematic Global Positioning System unit. The reservoir was mapped by boat using a single-beam echosounder and RTK GPS. The point density varied based on morphologic variability and observation method from a high of 1.5 pts. per m^2 to a low of 1 pt. per 9 m^2.

A synthetic (aka virtual) topography with TPCs was built on the original channel elevation (Fig. 5B). The topographic control consists of two nozzles (TPC1 & TPC2) and one oversized landform. The designs of the TPCs require a gross sediment fill and cut of 337,956 and 66,532 m^3, respectively, yielding a net fill of 271,424 m^3 (Fig. S1). These values indicate that substantial additional material would need to be brought in to enable the re-contouring, which could be accomplished by simply waiting for more reservoir sedimentation to take place at OHD. As a result, the design represents a long-term management plan for reservoir sedimentation at OHD without requiring any removal and off-site storage. Because mountain reservoirs typically have coarsening upward depositional sequences topped with gravel and/or cobble, with even coarser bed material in any distributary channels, it seems theoretically feasible to manage the available sediment stock to make the best use of each size fraction where best suited from a geotechnical engineering viewpoint. The construction goal would be to disturb the sediment as least as possible, using as much of the in-place structure as possible. Details of exact construction opportunities and constraints, including sediment mixology, will significantly vary by setting.

TPC1 was designed to be a very strong nozzle, with significant width reduction and bed elevation increase. River width at TPC1 was reduced to 30 % of the original wetted width at the highest flow (407 m^3/s) during the simulation period. The height of TPC1 was set to be the highest flow depth (407 m^3/s) to have TPC1 not inundated by flows. In contrast, TPC2 involved modest re-contouring emphasizing effects for low flows, instead of for all flows. The low-flow width of the riverbed at TPC2 was reduced to 40 % of the original riverbed. The elevation on the left bank was increased by 3 m while the right bank was slightly elevated (1 m) because of the feature of topography. Between the two nozzles, a natural topographic expansion exists, yielding an oversized landform. Its bed elevation was reduced by 3 m to mimic the condition when the deposited sediment is removed, and then that material could be used to build the TPCs instead of bringing in material from elsewhere.

3.3. 2D hydrodynamic modelling

The commercial software TUFLOW HPC was used to simulate the steady-state 2D (depth-averaged) Shallow Water Equations (WBM, 2018) for observed and theoretical/exploratory DEMs. Lateral and longitudinal velocity patterns were essential to answer study questions, while vertical ones were not needed given the relatively low height of the reservoir, the constricted canyon, and the dominance of 2D flow during floods.

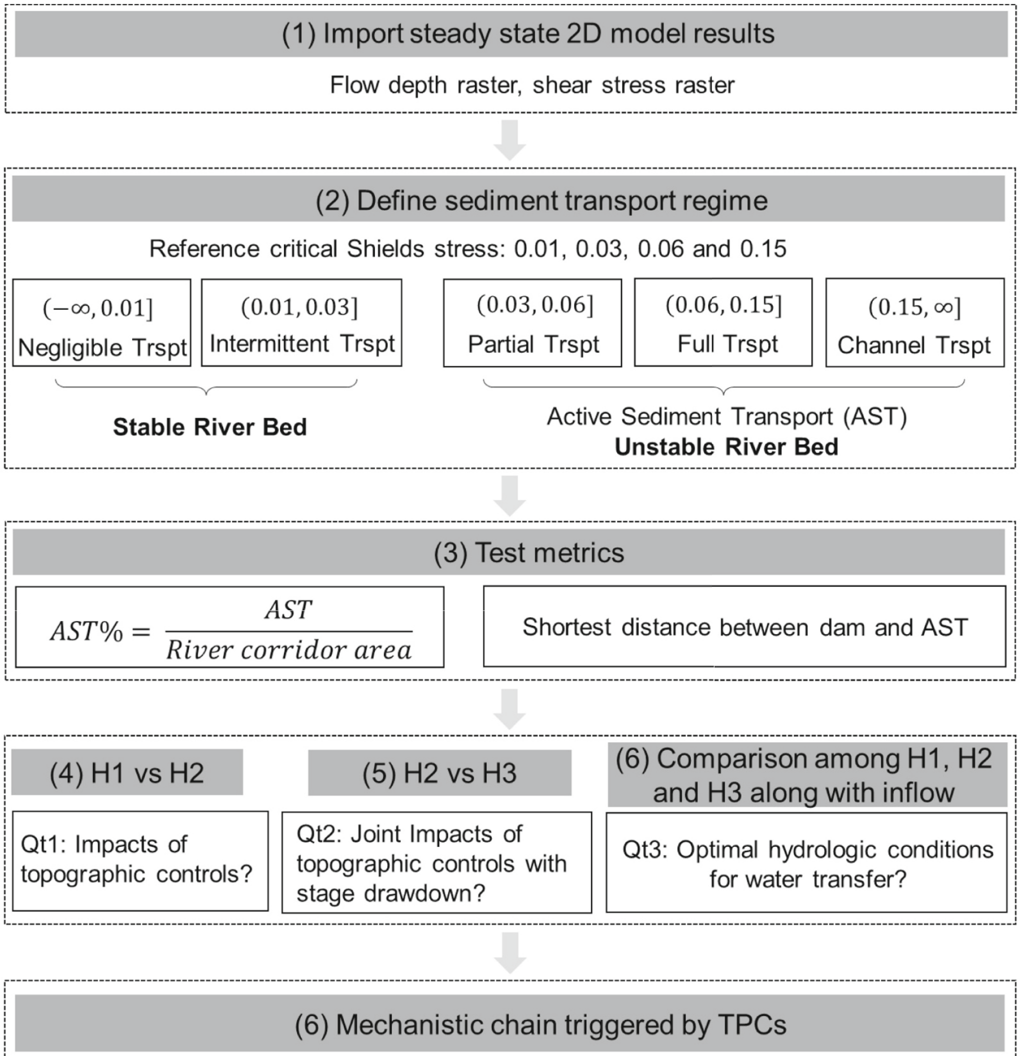

Fig. 4. Data analysis framework developed in this study.

Table 1
Exploratory scenarios to answer study questions.

Scenario	Scenario name	Design conceptualization
H1	Original topography	The reference scenario is based on recent topographic mapping and hydrological data.
H2	Topographic control	Two topographic nozzles (TPC1 & TPC2) were built into the study reach.
H3	Topo-hydro control	Three reservoir WSE scenarios were designed. H3–1 represents a minor WSE reduction (0.6 m). H3–2 represents a minor WSE increase (0.3 m). H3–3 represents a significant (25 %) WSE decrease (2.9 m).

3.3.1. Model parameters

Given extensive validation of 2D modeling elsewhere along the Yuba River with similar bed material, topography, and hydraulics, turbulence-closure and flow-resistance parameter values were taken from those past studies (e.g., Barker et al., 2018). The TUFLOW Smagorinsky viscosity method was used for turbulence closure with a coefficient value of 0.5 and a constant value of 0.005 m^2/s. Given predominantly gravel and cobble alluvium, Manning's n value was 0.04 (Fig. 3).

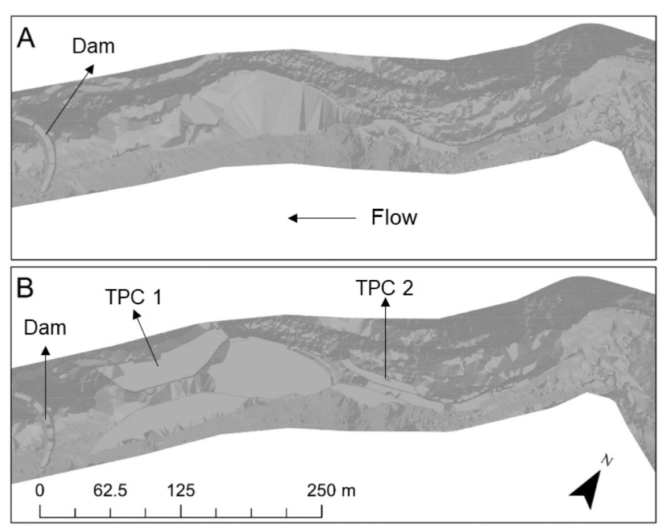

Fig. 5. Hillshade terrain visualization emphasizing shape over elevation. (A) 2018 river topography. (B) synthetic design.

3.3.2. Flow simulations

Steady-state in-channel flows were simulated to evaluate how sediment erosion would respond to topography and WSE under a constant flux of water with the sediment load it can carry, and thus to know what events can cause the designated pattern and magnitude of sediment erosion. Among the 18 flows simulated, three representative in-channel flows (Table 2) were selected with Spearman correlation and flow frequency analysis to focus on herein. Floods were not considered in this study, because during floods the reservoir's WSE reaches and exceeds the spillway crest elevation (619 m), which makes WSE adjustment impossible, and WSE manipulation was one of the interesting topics of inquiry. Further, the focus of this study is on the management of sediment influx and redistribution within the reservoir during lower to moderate flows that necessitate expensive, frequent maintenance operations.

3.3.3. Model performance

TUFLOW HPC is a well-developed model that has been extensively validated for use along the Yuba River (Hopkins and Pasternack, 2018; Pasternack, 2023). Given the remote and extremely hazardous conditions in the river during even modest flows at this study site, most model validation of hydraulics with the baseline topography was infeasible except for comparing modeled and observed WSEs at the dam crest. In fact, comparing WSE is the common strategy for validating lake/reservoir hydrodynamic models, if any validation is done at all (Kouassı et al., 2013; Castillo et al., 2015). As a result, the study is in the realm of scientific exploration and not predictive forecasting with high certainty, using the uncertainty terminology and concepts of Murray (2003).

3.4. Test metrics

The introduction presented a hypothesized hydro-morphodynamic mechanism that would be instituted by re-contouring the river. Mechanistic modeling is capable of characterizing how the river's hydraulics ought to respond to the designed change in topographic steering. This study implemented two specific test metrics that quantify the magnitude of difference among scenarios H1, H2, and H3.

3.4.1. Sediment erosion capability

The first metric identified areas of active scour in each simulation, because the hypothesized conceptual model of the TPCs functioning requires that active scour be focused in the vicinity of the TPCs. The first step involved estimating where flow had the capability to scour sediment (and/or route sediment through without depositing) in the OHD backwater zone. Bed shear stress (Eq. (1)) was converted into non-dimensional Shields stress (Eq. (2)) to make results comparable across all scenarios:

$$\tau_b = \rho g V^2 n^2 / h^{1/3} \tag{1}$$

$$\tau^* = \tau_b / (\rho_s - \rho_w) g d \tag{2}$$

where ρ_w is water density, ρ_s is bed particle bulk density, g is gravity, d is the representative bed material grain size, n is Manning's resistance parameter, V is flow velocity, h is flow depth, τ_b is bed shear stress, and τ^* is Shields stress.

Next, instead of calculating a specific sediment transport rate, which can be highly uncertain, local Shields stress (τ^*) values were categorized/aggregated into less uncertain sediment transport regimes defined by Lisle et al. (2000), where values of $\tau^* < 0.01$ correspond to negligible transport, $0.01 < \tau^* < 0.03$ correspond to intermittent entrainment, $0.03 < \tau^* < 0.06$ corresponds to partial transport (Wilcock et al., 1996), $0.06 < \tau^* < 0.15$ corresponds to full transport, and $\tau^* > 0.15$ corresponds to channel alteration. Intermittent transport indicated disturbances exist to the substrate of benthic organisms, but not necessarily to sediment movement, and there can even be deposition during this regime (Sawyer et al., 2010). Partial transport implies some over-ample and over-exposed particles of a given size on the bed surface area are active while others of the same size are immobile. Full transport implies a consistent 'conveyor belt' of sediment transport along the bed, up to two grains thick. Channel alteration transport indicates an increased scour potential compared with that in full transport, possibly with riverbed reconfiguration. Thus, 2D modeling is only used to predict which regime a location is in, which is an easier, less uncertain goal than predicting sediment transport rates explicitly.

Finally, to further simplify erosion analysis and reduce uncertainty, partial, full and channel alteration transport regimes were combined to obtain the active sediment transport regime (AST) mapped with polygons that represented unstable riverbed, assuming the same bed material everywhere. The normalized-areal coverage of AST (A_{st}, Eq. (3)) was used as the test metric to evaluate flow scour capability throughout the model domain, especially looking for its occurrence in the vicinity of the TPCs. Meanwhile, area covered by negligible and intermittent transport regimes were assumed to be stable riverbeds, and likely areas for sediment deposition.

$$A_{st} = \frac{(A_p + A_f + A_c)}{TA_{H1}} * 100\% \tag{3}$$

A_p, A_f, A_c are the areal coverage of partial, full and channel alteration regimes, respectively. A_{st} is the areal coverage of AST normalized by the maximum total wet area in H1 (TA_{H1}=14,985 m^2). A_{st} values of 0 and 100 % indicate stability or instability, respectively, for the whole channel. This approach evaluates sediment transport capacity of water, so it is independent of sediment supply. It is reporting the potential for what could happen to sediment in the study area.

3.4.2. Shortest AST-to-dam distance

The second metric identified the shortest distance between the active scour area (AST coverage ≥40 %) and the dam. This metric was used to compare scenarios H2 and H3 against the reference scenario H1 to determine if they kept sediment dynamics farther upstream. This metric is important, because one concern with reservoir sedimentation is that sediment eroded in the backwater zone will transport downstream and deposit in front of the sediment wedge, eventually impacting dam infrastructure – or outright depositing at the dam if velocities are high enough to enable that. Meanwhile, intense erosive stresses against the dam could also be problematic for any infrastructure present.

To map the AST longitudinal profile, 102 cross-sectional rectangles with the same width were spaced along the corridor's centerline using River Bathymetry Toolkit (ESSA, 2019). The river corridor spatial domain was set based on the maximum wet area in H1 and the bank extended from that to where the vegetation started to intensively occur (Thorne et al., 2005). The percentage of AST coverage within each cross-sectional rectangle was calculated by dividing AST coverage in each rectangle by the rectangle's area. The area of the cross sections ranges from 117 to 401 m^2.

3.5. How questions were answered

To answer Qt1, about the impacts of topographic controls on the foci

Table 2
Flow regime of steady-state flow runs in OHD site.

Flow regime	Flow range (m^3/s)	Frequency of daily occurrence	Selected flow event (m^3/s)
Base channel flow	[0, 8.5]	[30 %, 70 %]	2.5
Medium flow	[8.5, 31]	[5 %, 30 %]	9.4/17
High flow	[31, 85]	[1 %, 5 %]	83
Flood flow	[>85]	[−∞, 1 %]	None

of sediment erosion, the normalized differences of AST and shortest distance were calculated (as percent) between scenarios H1 and H2 (reference scenario: H1) (Eq. (4)).

$$\text{Metric variance} = \frac{\left(\text{Metric}_2 - \text{Metric}_{\text{reference}}\right)}{\text{Metric}_{reference}} * 100\% \tag{4}$$

where "metric" refers to AST or shortest distance. The normalized difference of the shortest distance in H1 and H2 was used to evaluate how the re-contouring impacts sediment erosion in the TPCs and upstream areas. Normalized difference percent values for either metric <30 % were interpreted to indicate small impacts, while values >60 % were interpreted to indicate large impacts. Beside the normalized difference percent metrics, the location, size, centroid and shape of AST were used to evaluate the impact of TPCs on the pattern of sediment erosion with a visual check.

The same protocol was followed to answer Qt2 about impacts of topographic controls with WSE drawdown on the sediment erosion pattern. H2 was set to be the reference scenario. Comparisons of metrics between H2 and H3–1 were used to estimate how small WSE adjustment performed while H2 and H3–3 evaluated how the large WSE adjustment affected sediment erosion.

To answer Qt3, finding the optimal hydrologic conditions for the designed topographic controls, the two normalized difference percent metrics were evaluated along with upstream discharge. H1 was set to be the reference scenario. A comparison of metrics between H1 and H2 was used to infer how TPCs performance varies along with the upstream flow. A comparison between H1 and H3 was used to infer the impact of WSE adjustment on TPCs in different hydrologic conditions.

4. Results

4.1. Sediment erosion with original topography

The distribution of sediment transport regimes in the existing topography displayed a spotty pattern in response to the presence of natural landform constrictions and large bed elements that impose topographic steering (Fig. 6). Beginning at base flow, AST occurred mainly in riffle-pool units and secondarily at bedrock outcrops. As inflow increased, the areal percentage of AST expanded upstream and downstream. When inflow was in the medium flow regime, independent AST patches coalesced, forming elongated erosion zones along the river bends similar in size and shape to medial and point bars observed as landforms in the reservoir and its backwater zone. When inflow was in the high flow regime, these elongated erosion zones coalesced making the entire river fully activated for sediment transport.

As for different grain sizes, all sizes exhibited more sediment transport capacity as discharge increases, but there was a significant difference in the amount of full transport and channel alteration regimes among the five sizes evaluated (Fig. S2). Further, the occurrence of sediment erosion patterns differed (see map set in the supplementary materials file). For grain size ≤32 mm, a spotty sediment erosion pattern occurred across all flow events because of the high sensitivity of smaller gravel sizes to lower bed shear stresses. Furthermore, the presence of large gravel bars in the backwater zone submerged new terrain, resulting in the creation of new AST areas with increasing discharge. On the other hand, for grain size >32 mm, the river's capability to transport coarse gravel was limited, except in the flood regime. The sensitivity analysis indicated that AST variation reached a breakpoint at 32 mm. For grains <32 mm, <30 % of the area was occupied by negligible transport regime, while for those >32 mm, the negligible and intermittent transport regimes dominated the entire study reach (>50 %).

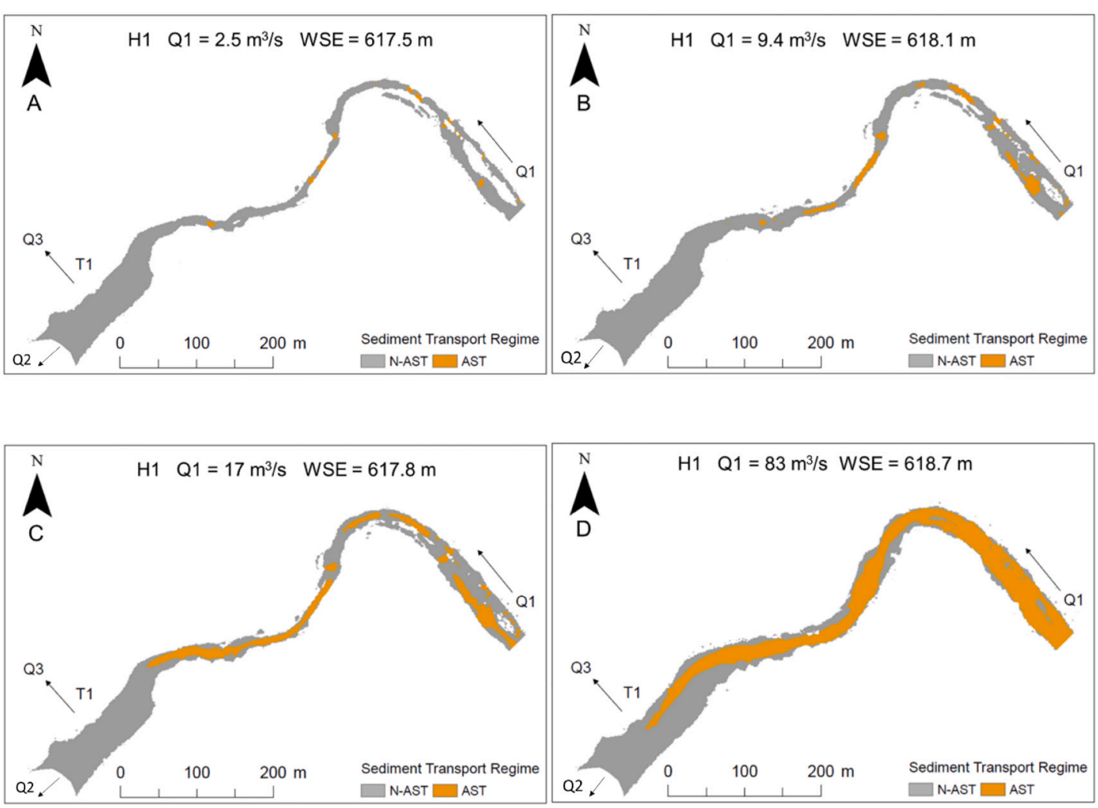

Fig. 6. Spatial distribution of the sediment transport regimes in H1 of grain size 32 mm. Q1 is the Middle Yuba River inflow, Q2 is OHD outflow, Q3 is flow diverted through the tunnel. AST is the active sediment transport zone. N-AST is the non-active sediment transport zone. Flow is from upper right to lower left, with the dam at the end of the fill color in the lower left.

And the channel alteration regime almost disappeared for these larger grain sizes. Therefore, bed material sizes >32 mm are recommended for constructing and armoring stable nozzles at OHD.

4.2. Sediment erosion with topographic controls

Spatially, constructed nozzles had significantly increased sediment erosion potential over their area for the grain sizes investigated, while they functioned to reduce sediment erosion potential upstream and downstream. In the base and medium flow regimes (Fig. 7A), TPC2 was fully erosional, indicated by the full coverage of AST (>90 %). Meanwhile, AST coverage upstream of TPC2 dropped from 75 % to zero because of the increased backwater effect caused by TPC2. Downstream of TPC2, AST coverage reduced from 60 % to zero compared with that in the same area in H1. As inflow increased, the areal coverage of AST in TPC2 increased and expanded to its upstream until it connected to the other AST patch, while the area downstream of the oversized landform was not eroded until MYR reached the high flow regime (Fig. 7B).

As for the shortest distance between the dam and AST, adding TPCs caused mild hydraulics upstream in the base and medium flow regimes (Table S2), which is interpreted to support sediment deposition there. In the high flow regime shortest distance was reduced. In the base flow regime, AST occurred in front of the dam in both H1 and H2. Adding TPCs had a limited impact on the distancing of sediment erosion to the dam. In the medium flow regime, adding TPCs reduced sediment erosion near the dam, which would help keep the low-lying intake structure stable. The shortest AST-to-dam distance was reduced on average by 66 m. As flow keeps increasing, sediment erosion near the reservoir was largely increased. The distance in H2 was reduced by 97 m on average. This indicates that the mechanism is flow-dependent, which is meaningful for carefully designing topographic steering to obtain whatever outcome is desired for each flow.

4.3. Sediment erosion with topographic control and WSE adjustment

Compared with H2, reducing reservoir WSE (H3−1) by 0.6 m enhanced sediment erosion in TPC1 while the area near TPC2 was not affected. During base flow, no AST coverage was observed in TPC1 in H3–1. During medium flow, AST was observed near TPC1. As upstream flow increases within the regime, the areal coverage of AST in TPC1 was enhanced, expanding from the TPC1 center to its upstream and downstream. When the upstream inflow Q1 increased to a high flow regime, TPC1 was fully activated (Fig. 8A). The impact of stage drawdown on sediment erosion in TPC1 was positively related to the reduction of water level. Similarly, in H3–3, AST occurred at the end of TPC1 near the reservoir in the base flow regime. Then the erosion zone expanded upstream as the MYR inflow increased. TPC1 was fully activated during medium flow in H3–3.

To determine the impact of increasing WSE, an AST comparison was conducted between H3–2 and H3–1. In the base flow regime, increasing WSE by 0.9 m had limited impacts on AST coverage because of the low initial AST coverage. However, during medium flow, AST in TPC2 shrank to its center and disappeared in TPC1. As upstream inflow increased to the high flow regime, increasing WSE did not change the

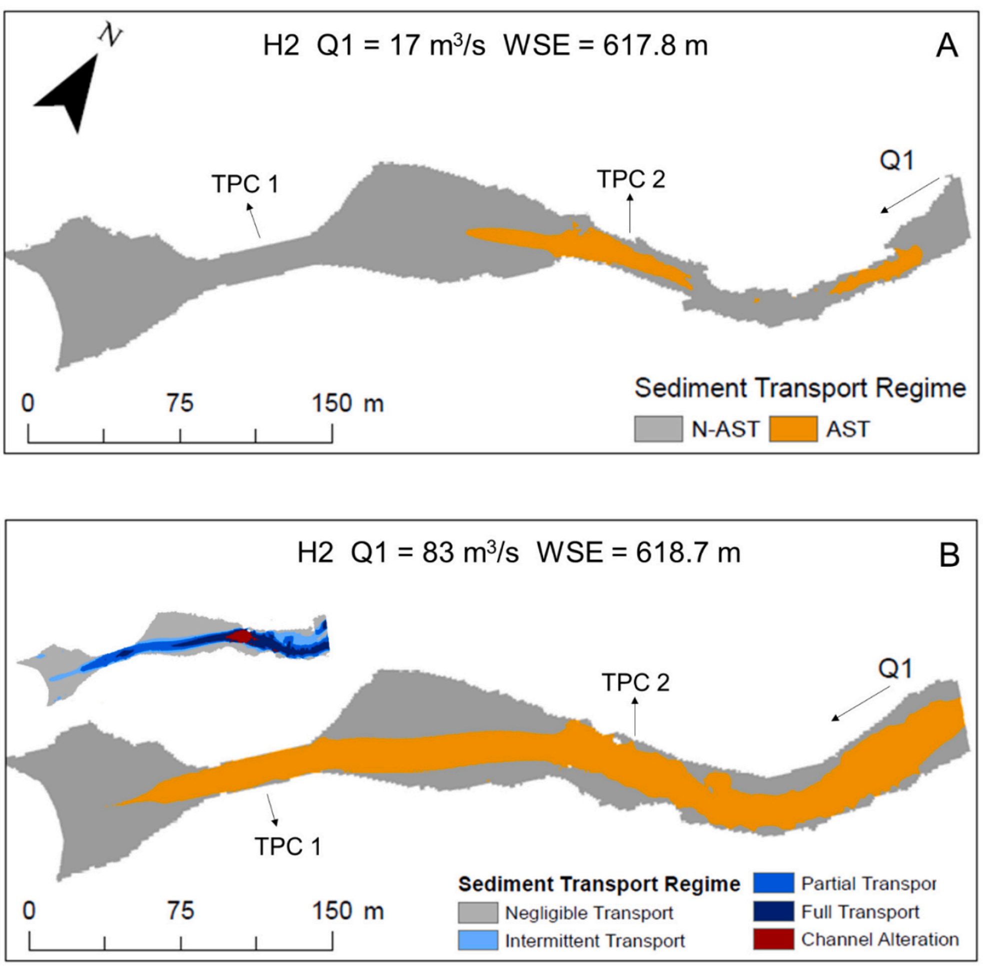

Fig. 7. Spatial distribution of the sediment transport regimes of medium and high flow regimes in H2. Inset map in (B) shows more detailed sediment transport regimes for the same area.

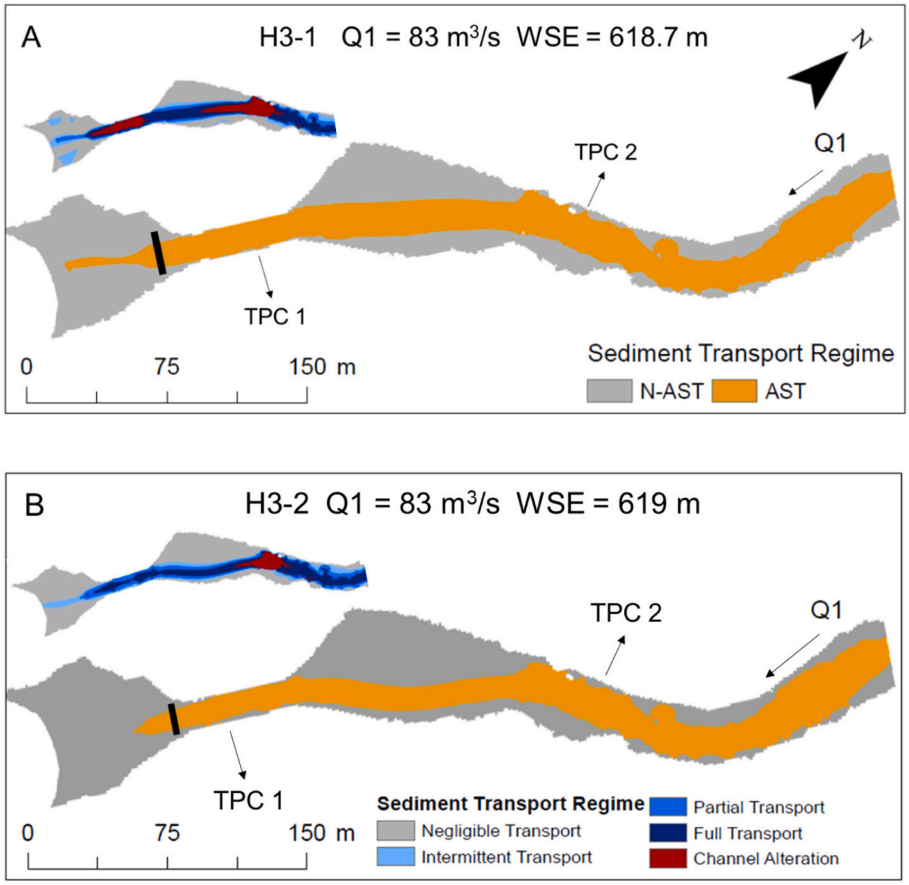

Fig. 8. Spatial distribution of sediment transport regimes of medium flow regime in H3–1 and H3–2. Q1 is Middle Yuba River inflow. The black rectangle indicates the starting point of the distance between the dam and AST cross section. Inset maps show more detailed sediment transport regimes for the same area.

AST coverage (yellow area) significantly (Fig. 8). H3–1 and H3–2 both had active TPCs and similar AST coverage. However, zooming in on the sediment transport regime composition of AST, the proportion of AST changed significantly. Specifically, the channel alteration regime (red area) in TPC1 in H3–1 downgraded to the full transport regime (dark blue) in H3–2. Meanwhile, in TPC2, the coverage of the channel alteration regime still appeared but with less coverage.

Minor WSE adjustment (<1 m) had a limited impact (<5 %) on the AST-to-dam distance for all flow regimes. However, reducing WSE by ¼ of the adjustable range (2.9 m) had a significant impact on the AST-to-dam distance. On average, reducing WSE by 2.9 m reduced the distance by 66 %. During both base and medium flow regimes, distance normalized difference (Eq. (4)) caused by WSE adjustment was similar. Meanwhile, distance normalized difference was lowest (23 %) during the high flow regime for all scenarios.

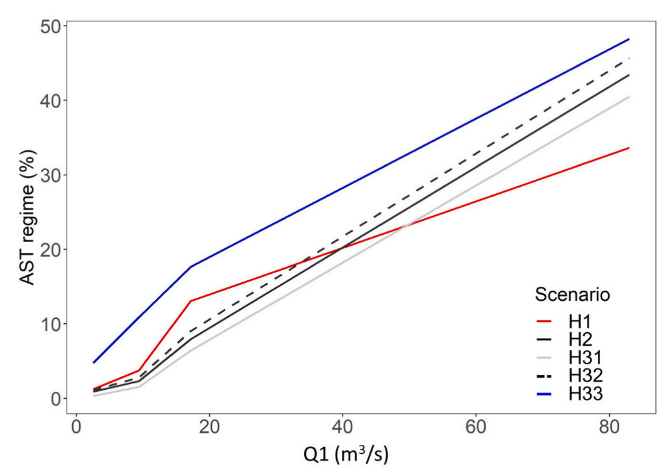

Fig. 9. Areal percentage of AST of four scenarios along with upstream inflow-MYR (Q1).

5. Discussion

5.1. Question 1: impacts of topographic constrictions

Adding nozzles to the channel enhanced the area of sediment erosion during high in-channel flows while reducing it during lower flows (Fig. 9). In the baseflow regime, differences in AST among scenarios were ≤5 %, likely because inflow was too small to scour sediment. Thus, neither adjusting topography nor hydrology altered sediment erosion significantly for baseflow.

In the medium flow regime, AST coverage with topographic constrictions, except for scenario H3–3, was lower than that of H1. The AST coverage in H2 was ~40 % lower than that in H1. As discharge increased, AST coverage in design scenarios surpassed that in the reference scenario. AST in H2 was 29 % higher than in H1. The oversized landform acted as a buffer zone to reduce sediment erosion upstream of it in the low and medium flow.

In the high flow regime, TPC2 was submerged, and the backwater effect was defeated by high inflow. Therefore, TPC1 accelerated flow and thus is interpreted to have increased sediment erosion potential greatly as long as bed material was left unarmored in construction. This study explored broad scientific principles and did not undertake iteratively engineering a final design, such as to control flood effects. A better outcome is achievable in design refinement by iteratively adjusting the length of the oversized landform and the heights of the nozzle landforms.

Spatially, adding TPCs slowed the river upstream in the base and medium flow regimes, which is interpreted to promote deposition upstream under those conditions, but reduced distance in high flow regime, which is indicated by a large negative value in Table 3. Because of the low flow and relatively high backwater effect, the current version of TPCs was able to drive sedimentation upstream of TPC2 and reduce sediment dynamics near the dam. In this way, hydraulic or mechanical excavation can be economically and predictably established in this location to constantly remove just new incoming sediment. However, instead of reducing sediment dynamics near the dam, TPCs in high flow acted as accelerators of sediment transport. The distance between the sediment erosion area and the dam was largely reduced. If holding sediment erosion away from the dam is an important design specification, then the depth of the oversized landform between TPCs (and/or possibly the height of the nozzle crests) should be increased to increase its backwater effect and thereby institute stronger functioning as a settling basin. If increasing sediment erosion to have sediment transport over/through the dam is the goal, the current version of TPCs would be a good example for other rivers.

5.2. Question 2: role of WSE adjustment

The area affected by minor WSE adjustment ≤ 1 m was in the vicinity of TPC2. Reducing reservoir WSE would increase sediment erosion near TPC2 and route more sediment through TPC2 into the oversized landform. Increasing WSE tends to pond sediment upstream of TPC1, reducing sediment erosion in both TPC1 and the oversized landform. However, reducing WSE significantly would fully activate TPC2 but also trigger sediment erosion in TPC1. The oversized area had zero AST coverage during base and medium flow, implying little sediment would be routed to TPC1. However, sediment already deposited in TPC1 would be eroded and transported to the dam even during baseflow. In addition, the performance of WSE adjustment is flow dependent. The highest normalized difference of AST caused by WSE adjustment always occurred during baseflow. As flow increased, AST normalized difference decreased, because during high flow, sediment was highly eroded even when WSE was high. Therefore, adjusting WSE in a high flow regime led to a relatively small, normalized difference in AST.

5.3. Question 3: optimal hydrologic conditions for topographic constriction

Given the design used herein, the medium flow with a minor WSE adjustment is recommended as the optimal range of hydrologic conditions for TPCs for any one of several options for sedimentation management that can be implemented relatively frequently and at a lower cost compared with large-scale, expensive mechanical excavation and storage of removed sediment elsewhere. Even though AST coverage in TPC scenarios was lower than that in the reference scenario, sediment erosion occurred in the designated focused area upstream and downstream of TPC2 where acceleration and deceleration are theorized by FCR. The reduction in AST occurred in the oversized area that was originally covered by AST. This reduction of AST was expected by the hypothesis, and that could be paired with the outfitting of the flank of the oversized landform with infrastructure to enable localized hydraulic/mechanical excavation.

The normalized difference in AST between TPCs scenarios and the reference scenario was small (<5 %) during the base flow because the base flow was too small to entrain sediment, not to mention having TPCs function. While during high flow, the AST coverage in TPCs scenarios surpassed that in the reference scenario, TPCs can lead to more sediment erosion near the dam because of the narrowed channel width of TPC1. Given that OHD is only 21 m high, eroded sediment of mixed sizes might potentially be able to spill over it, but that would require additional research at that site, and generally on a case-by-case basis to evaluate if erosion potential near the dam should be a concern, a benefit, or irrelevant. Besides the excessive sediment erosion near the dam, the high flow outweighed the impact of minor WSE adjustment on the distance of AST to the dam. To control the distance of sediment erosion to the dam, large WSE adjustment is needed.

Table 3
Distance normalized difference in percent (Eq. (4)) among scenarios. H2 ~ H1 means comparison between H2 and H1. H# ~ H2 means the comparison between H# and H2, where # is 31, 32 or H33.

Q1 (m^3/s)	H2 ~ H1	H31 ~ H2	H32 ~ H2	H33 ~ H2
2.5	−2	−2	5	−81
9.4	12	−2	3	−81
17.2	−30	−2	4	−82
83.0	71	0	8	−23

6. Conclusions

This numerical experimentation study tested the performance of constructed topographic controls in assisting the sedimentation management of the sand, gravel, and cobble fractions of bedload at the upstream end of a reservoir in a remote, confined mountain canyon. Sediment transport regimes were divided into stable and unstable domains over the riverbed by a reference value of non-dimensional shear stress of 0.03. The areal coverage and location of unstable riverbed patches were analyzed to evaluate the redistribution of deposited sediment triggered by nozzles and oversized landforms. The results found that topographic re-contouring of reservoir landforms performed well at redistributing sediment erosion and deposition in a controlled fashion. In the medium flow regime, the unstable riverbed coverage was reduced by 18 % on average with topographic controls. Adjusting the water stage can effectively alter sediment dynamics near the dam. Specifically, reducing WSE can enhance sediment erosion and can yield more sediment erosion in oversized landforms, while increasing WSE can enhance the backwater effect so that more sediment tends to deposit and stay upstream of nozzles.

This work explored the possibility of extending the life of dams with a capacity of holding $\sim 10^5$ m^3 of sediment in lieu of dam removal, especially for conditions when sediment flushing is not possible or the cost is too high. The study provides both short-term and long-term management insights for small dams in managing sedimentation with topographic steering, and firstly applied the feedback between flow and sediment to change the sediment dynamism spatially. However, the details of what is possible depend on local site conditions. Exactly where a dam operator wants to focus erosion or deposition may vary. Thus, one of the main contributions of this study is to present the theoretical concept of controlling foci of erosion and deposition and explore the concept's potential, with the goal of serving as a pivot study for real-world sedimentation management practices.

Declaration of competing interest

The authors declare the following financial interests/personal relationships which may be considered as potential competing interests: Gregory Pasternack reports financial support was provided by Yuba Water Agency. Gregory Pasternack reports financial support was provided by National Institute of Food and Agriculture. Senior author has done paid consulting work for Yuba Water Agency on unrelated topics in other parts of the Yuba River. He has never consulted on reservoir sedimentation in general or specifically on any issues at the dam used as the test site in this study.

Data availability

Data will be made available on request.

Acknowledgments

This study was primarily funded by Yuba Water Agency [award number 201016094]. This project was also supported by the USDA National Institute of Food and Agriculture, Hatch [project number CA-D-LAW-7034-H]. We also thank Profs. Peng Gao (Syracuse) and Sam Sandoval-Solis (UC Davis) for constructive reviews of the manuscript prior to journal submission. We thank the peer reviewers for constructive feedback and insights that significantly improved the writing.

Appendix A. Supplementary data

Supplementary data to this article can be found online at https://doi.org/10.1016/j.geomorph.2023.108882.

References

Barker, J., Pasternack, G.B., Bratovich, P., Duane, M., Wyrick, J.R., Johnson, T., 2018. Kayak drifter surface velocity observation for 2D hydraulic model validation. River Res. Appl. 34 (2), 124–134.
Blanckaert, K., 2011. Hydrodynamic processes in sharp meander bends and their morphological implications. J. Geophys. Res. Earth Surf. 116 (F1).
Brown, R.A., Pasternack, G.B., 2014. Hydrologic and topographic variability modulate channel change in mountain rivers. J. Hydrol. 510, 551–564.
Brown, R.A., Pasternack, G.B., Lin, T., 2016. The topographic design of river channels for Form-Process linkages. Environ. Manag. 57 (4), 929–942.
Byrne, C.F., Pasternack, G.B., Guillon, H., Lane, B.A., Sandoval-Solis, S., 2020. Reach-scale bankfull channel types can exist independently of catchment hydrology. Earth Surf. Process. Landf. 45 (9), 2179–2200. https://doi.org/10.1002/esp.4874.
Byrne, C.F., Pasternack, G.B., Guillon, H., Lane, B.A., Sandoval-Solis, S., 2021. Channel constriction predicts pool-riffle velocity reversals across landscapes. Geophys. Res. Lett. 48 (20), e2021GL094378.
CAL FIRE, 2022. Historic fire perimeters. Retrieved from. https://www.fire.ca.gov/what-we-do/fire-resource-assessment-program/fire-perimeters (Accessed 06 2023).
Castillo, L.G., Carrillo, J.M., Álvarez, M.A., 2015. Complementary methods for determining the sedimentation and flushing in a reservoir. J. Hydraul. Eng. 141 (11), 05015004.
Coleman, J.M., 1976. Deltas-Processes of Deposition and Models for Exploration. Continuing Education Publication Company, Champaign, IL.
Collison, A., 2016. Restoring the Napa River: lessons learned from a long term private-public project. Environmental Science Associates, powerpoint presentation. https://www.calandtrusts.org/wp-content/uploads/2016/06/The-Napa-River-Restoration-Project.pdf (Accessed 06 2023).
Curtis, J.A., Flint, L.E., Alpers, C.N., Yarnell, S.M., 2005. Conceptual model of sediment processes in the upper Yuba River watershed, Sierra Nevada, CA. Geomorphology 68 (3–4), 149–166.
Dettinger, M., 2011. Climate change, atmospheric rivers, and floods in California – a multimodel analysis of storm frequency and magnitude changes. J. Am. Water Resour. Assoc. 47 (3), 514–523.
EPA, 2020. "United States Environmental Protection Agency. Napa river restoration: basis of design: Oakville to Oak Knoll Reach, working version 4." Prepared for County of Napa. https://www.epa.gov/sfbay-delta/napa-river-restoration-project-oakville-oak-knoll-reach-group-c-site-14 (Accessed 12 2020).
ESSA, 2019. River Bathymetry Toolkit (RBT). https://portal.opentopography.org/tools/viewTool?toolId=81 (Accessed 01 2019).
Fites-Kaufmann, J.A., Rundel, P., Stephenson, N., Weixelman, D.A., 2007. Montane and subalpine vegetation of the Sierra Nevada and Cascade Ranges. In: Barbour, M.G., Keeler-Wolf, T., Schoenherr, A.A. (Eds.), Terrestrial Vegetation of California, 3rd ed. University of California Press, Berkeley.
Fryirs, K., 2013. (Dis) Connectivity in catchment sediment cascades: a fresh look at the sediment delivery problem. Earth Surf. Process. Landf. 38 (1), 30–46.
Gilbert, G.K., 1917. Hydraulic-mining Debris in the Sierra Nevada. U.S. Geol. Survey Prof. Paper, 105 (Washington, D.C.) (154 pp).
Ho, M., Lall, U., Allaire, M., Devineni, N., Kwon, H.H., Pal, I., Raff, D., Wegner, D., 2017. The future role of dams in the United States of America. Water Resour. Res. 53 (2), 982–998.
Hooke, J., 2003. Coarse sediment connectivity in river channel systems: a conceptual framework and methodology. Geomorphology 56 (1–2), 79–94.
Hopkins, C.E., Pasternack, G.B., 2018. Autumn 2014 Lower Yuba River TUFLOW GPU 2D Model Description and Validation. Prepared for Yuba County Water Agency. University of California, Davis, CA.
Hotchkiss, R.H., Parker, G., 1991. Shock fitting of aggradational profiles due to backwater. J. Hydraul. Eng. 117 (9), 1129–1144.
Julien, P.Y., 2010. Erosion and sedimentation. Press, New York.
Kouassı, K.L., Kouame, K.I., Konan, K.S., Sanchez Angulo, M., Deme, M., Meledje, N.D.H.E., 2013. Two-dimensional numerical simulation of the hydro-sedimentary phenomena in Lake Taabo, Côte d'ivoire. Water Resour. Manag. 27, 4379–4394.
Lewis, D.J., Singer, M.J., Dahlgren, R.A., Tate, K.W., 2006. Nitrate and sediment fluxes from a California rangeland watershed. J. Environ. Qual. 35 (6), 2202–2211.
Li, T., Pasternack, G.B., 2022. Water transfer redistributes sediment in Small Mountain Reservoirs. Water Resour. Manag. 36 (13), 5033–5048.
Liro, M., 2015. Gravel-bed channel changes upstream of a reservoir: the case of the Dunajec River upstream of the Czorsztyn Reservoir, southern Poland. Geomorphology 228, 694–702.
Liro, M., 2016. Development of sediment slug upstream from the Czorsztyn Reservoir (southern Poland) and its interaction with river morphology. Geomorphology 253, 225–238.
Lisle, T.E., Nelson, J.M., Pitlick, J., Madej, M.A., Barkett, B.L., 2000. Variability of bed mobility in natural, gravel-bed channels and adjustments to sediment load at local and reach scales. Water Resour. Res. 36 (12), 3743–3755.
Litschert, S.E., MacDonald, L.H., 2009. Frequency and characteristics of sediment delivery pathways from forest harvest units to streams. For. Ecol. Manag. 259 (2), 143–150.
MacWilliams Jr., M.L., Wheaton, J.M., Pasternack, G.B., Street, R.L., Kitanidis, P.K., 2006. Flow convergence routing hypothesis for pool-riffle maintenance in alluvial rivers. Water Resour. Res. 42 (10).
Maselli, V., Pellegrini, C., Del Bianco, F., Mercorella, A., Nones, M., Crose, L., Guerrero, M., Nittrouer, J.A., 2018. River morphodynamic evolution under dam-induced backwater: an example from the Po River (Italy). J. Sediment. Res. 88 (10), 1190–1204.
Morris, G.L., Fan, J., 1998. Reservoir Sedimentation Handbook: Design and Management of Dams, Reservoirs, and Watersheds for Sustainable Use. McGraw Hill Professional, New York.
Murray, A.B., 2003. Contrasting the goals, strategies, and predictions associated with simplified numerical models and detailed simulations. Geophys. Monogr.-Am. Geophys. Union 135, 151–168.
Nelson, A., Dubé, K., 2016. Channel response to an extreme flood and sediment pulse in a mixed bedrock and gravel-bed river. Earth Surf. Process. Landf. 41 (2), 178–195.
Olsen, W.H., Wagenbrenner, J.W., Robichaud, P.R., 2021. Factors affecting connectivity and sediment yields following wildfire and post-fire salvage logging in California's Sierra Nevada. Hydrol. Process. 35 (1), e13984.
Pasternack, G.B., Gilbert, A.T., Wheaton, J.M., Buckland, E.M., 2006. Error propagation for velocity and shear stress prediction using 2D models for environmental management. J. Hydrol. 328, 227–241.
Pasternack, G.B., Baig, D., Weber, M.D., Brown, R.A., 2018a. Hierarchically nested river landform sequences. Part 1: theory. Earth Surf. Process. Landf. 43 (12), 2510–2518.
Pasternack, G.B., 2023. Draft 2017 Lower Yuba River TUFLOW HPC 2D Model Description, Validation, and Exploratory Simulations. Prepared for Yuba Water Agency. University of California, Davis, CA.
Pasternack, G.B., Baig, D., Webber, M., Brown, R.A., 2018b. Hierarchically nested river landform sequences. Part 2: bankfull channel morphodynamics governed by valley nesting structure. Earth Surf. Process. Landf. 43 (12), 2519–2532.
Pasternack, G.B., Gore, J., Wiener, J., 2021. Geomorphic covariance structure of a confined mountain river reveals landform organization stage threshold. Earth Surf. Process. Landf. 46 (13), 2582–2606.
Ralph, F.M., Neiman, P.J., Wick, G.A., Gutman, S.I., Dettinger, M.D., Cayan, D.R., White, A.B., 2006. Flooding on California's Russian River: role of atmospheric rivers. Geophys. Res. Lett. 33, L13801.
Randle, T.J., Morris, G.L., Tullos, D.D., Weirich, F.H., Kondolf, G.M., Moriasi, D.N., Annandale, G.W., Fripp, J., Minear, J.T., Wegner, D.L., 2021. Sustaining United States reservoir storage capacity: need for a new paradigm. J. Hydrol. 602, 126686.
Rathburn, S., Wohl, E., 2003. Predicting fine sediment dynamics along a pool-riffle mountain channel. Geomorphology 55 (1–4), 111–124.
Sawyer, A.M., Pasternack, G.B., Moir, H.J., Fulton, A.A., 2010. Riffle-pool maintenance and flow convergence routing observed on a large gravel-bed river. Geomorphology 114 (3), 143–160.
Schumm, S.A., 1985. Patterns of alluvial rivers. Annu. Rev. Earth Planet. Sci. 13 (1), 5–27.
Senter, A.E., Pasternack, G.B., Piégay, H., Vaughan, M.C., 2017. Wood export prediction at the watershed scale. Earth Surf. Process. Landf. 42 (14), 2377–2392.
Thorne, C., Hey, R., Newson, M., 2005. Applied Fluvial Geomorphology for River Engineering and Management. Wiley.
Vaughan, M.C., 2013. Large Streamwood Storage Does Not Decrease Downstream through a Watershed (MS thesis). University of California, Davis, CA (61 pp).
WBM, 2018. TUFLOW Classic/HPC User Manual Build 2018–03-AD. WBM Oceanics Australia.
Wheaton, J.M., Brasington, J., Darby, S., Merz, J.E., Pasternack, G.B., Sear, D.A., Vericat, D., 2010. Linking geomorphic changes to salmonid habitat at a scale relevant to fish. River Res. Appl. 26, 469–486.
Wilcock, P.R., Kondolf, G.M., Matthews, W.G., Barta, A.F., 1996. Specification of sediment maintenance flows for a large gravel-bed river. Water Resour. Res. 32 (9), 2911–2921.
Yager, E.M., Venditti, J.G., Smith, H.J., Schmeeckle, M.W., 2018. The trouble with shear stress. Geomorphology 323, 41–50.
Yuba County Water Agency, 2014. Technical Memorandum 6-1: Riparian Habitat Upstream of Englebright Reservoir. Yuba River development project, FERC project no. 2246. Retrieved from. http://www.ycwa-relicensing.com/Technical%20Memoranda/Forms/AllItems.aspx (Accessed 06 2023).
Yuba County Water Agency, 2017. Log Cabin and Our House Diversion Dams Sediment Management Plan. Yuba River Development Project, FERC Project No. 2246.

Retrieved from. http://www.ycwa-relicensing.com/Technical%20Memoranda/Forms/AllItems.aspx (Accessed 06 2023).